

Large piezoelectric properties in KNN-based lead-free single crystals grown by a seed-free solid-state crystal growth method

Jie Yang, Faqiang Zhang, Qunbao Yang, Zhifu Liu, Yongxiang Li, Yun Liu, and Qiming Zhang

Citation: *Applied Physics Letters* **108**, 182904 (2016); doi: 10.1063/1.4948642

View online: <http://dx.doi.org/10.1063/1.4948642>

View Table of Contents: <http://scitation.aip.org/content/aip/journal/apl/108/18?ver=pdfcov>

Published by the *AIP Publishing*

Articles you may be interested in

Phase structure and piezoelectric properties of $(1-x)\text{K}0.48\text{Na}0.52\text{Nb}0.95\text{Sb}0.05\text{O}3-x(\text{Bi}0.5\text{Na}0.5)0.9(\text{Li}0.5\text{Ce}0.5)0.1\text{ZrO}3$ lead-free piezoelectric ceramics

J. Appl. Phys. **119**, 034101 (2016); 10.1063/1.4940191

Solid-state conversion of $(94-x)(\text{Na}1/2\text{Bi}1/2)\text{TiO}3-6\text{BaTiO}3-x(\text{K}1/2\text{Na}1/2)\text{NbO}3$ single crystals and their enhanced converse piezoelectric properties

AIP Advances **6**, 015310 (2016); 10.1063/1.4940662

Improvement of the piezoelectric properties in $(\text{K},\text{Na})\text{NbO}3$ -based lead-free piezoelectric ceramic with two-phase co-existing state

J. Appl. Phys. **117**, 214102 (2015); 10.1063/1.4921860

Largely enhanced electromechanical properties of $\text{BaTiO}3-(\text{Na}0.5\text{Er}0.5)\text{TiO}3$ lead-free piezoelectric ceramics

Appl. Phys. Lett. **105**, 082901 (2014); 10.1063/1.4893610

Effects of Li content on the phase structure and electrical properties of lead-free $(\text{Ag}0.85-x\text{Li}x\text{Na}0.1\text{K}0.05)\text{NbO}3$ piezoelectric ceramics

J. Appl. Phys. **111**, 054105 (2012); 10.1063/1.3692063



Searching? Trust CiSE.

Google Scholar search results for "python in scientific computing". The top result is "Python for scientific computing" by TE Oliphant, published in *Computing in Science & Engineering*, 2007. The snippet highlights that Python is an excellent scripting language for scientific computing and that with additional tools, it becomes a language suited for scientific and engineering code.

It's peer-reviewed and appears in the IEEE Xplore and AIP library packages.

Large piezoelectric properties in KNN-based lead-free single crystals grown by a seed-free solid-state crystal growth method

Jie Yang,^{1,2} Faqiang Zhang,¹ Qunbao Yang,^{1,a)} Zhifu Liu,¹ Yongxiang Li,^{1,a)} Yun Liu,³ and Qiming Zhang⁴

¹CAS Key Lab of Inorganic Functional Materials and Devices, Shanghai Institute of Ceramics, Chinese Academy of Sciences, Shanghai 200050, China

²University of Chinese Academy of Sciences, Beijing 100049, China

³Research School of Chemistry, The Australian National University, Canberra, ACT 2601, Australia

⁴Department of Electrical Engineering and Materials Research Institute, The Penn State University, University Park, Pennsylvania 16802, USA

(Received 14 December 2015; accepted 23 April 2016; published online 4 May 2016)

We report lead-free single crystals with a nominal formula of $(\text{K}_{0.45}\text{Na}_{0.55})_{0.96}\text{Li}_{0.04}\text{NbO}_3$ grown using a simple low-cost seed-free solid-state crystal growth method (SFSSCG). The crystals thus prepared can reach maximum dimensions of $6\text{ mm} \times 5\text{ mm} \times 2\text{ mm}$ and exhibit a large piezoelectric coefficient d_{33} of 689 pC/N. Moreover, the effective piezoelectric coefficient d_{33}^* , obtained under a unipolar electric field of 30 kV/cm, can reach 967 pm/V. The large piezoelectric response plus the high Curie temperature (T_C) of 432 °C indicate that SFSSCG is an effective approach to synthesize high-performance lead-free piezoelectric single crystals. *Published by AIP Publishing.* [<http://dx.doi.org/10.1063/1.4948642>]

Due to their extraordinary piezoelectric performance and non-toxic characteristic, potassium sodium niobate (KNN) based lead-free piezoceramics have attracted a great deal of attention since the work of Saito *et al.*¹ in 2004. Using the reactive templated grain growth (RTGG) method, the KNN-based textured piezoceramics can be synthesized with grains oriented in a preferred direction, usually $\langle 001 \rangle$. This will greatly improve the piezoelectric properties compared with the randomly oriented ceramics.² Therefore, one may expect that KNN-based single crystals (SC) along special orientations will generate even better piezoelectric properties than the textured ceramics, owing to their higher degree of orientation and grain-boundary-free microstructures.

Recently, a non-melting method, e.g., solid-state crystal growth (SSCG) method, has been developed to grow piezoelectric single crystals.^{3–5} In this method, a single crystal seed is tightly bonded to the polycrystalline ceramic matrix, and then, the target crystal will be grown by consuming the matrix when annealing at a suitable temperature below the melting point. It is found that not only the chemical compositions but also the crystalline orientations of the seed are crucial to the crystal growth.^{6,7} In the KNN case, only KTAO_3 crystal seed was found to be suitable for SSCG.^{8–10} However, high quality KTAO_3 single crystals are rather expensive, especially for the $\langle 110 \rangle$ -oriented ones. Therefore, it is attractive to develop a seed-free solid-state crystal growth method (SFSSCG) to grow high-performance KNN single crystals.

There have been constant efforts in growing single crystals through the solid-state crystal growth method without using extra crystal seeds. Using SiO_2 as an additive, Saldana *et al.*¹¹ controlled the exaggerated grain growth through adjusting sintering procedures, and successfully fabricated

dense BaTiO_3 single crystals. Wang *et al.*¹² prepared KNN single crystals sintered at 950 °C, using KNN nanoparticles and nanorods as starting materials, and the nanorods acted as the seeds. The crystals thus prepared can reach a maximum size of $\sim 3\text{ mm}$. Jiang *et al.*¹³ grew $\text{K}_{0.5}\text{Nb}_{0.5}\text{NbO}_3$ single crystals with dimensions of $11\text{ mm} \times 9\text{ mm} \times 3\text{ mm}$, using LiBiO_3 as a sintering aid. The single crystals show a d_{33} of 205 pm/V, which is much larger than that of the textured $\text{K}_{0.5}\text{Nb}_{0.5}\text{NbO}_3$ ceramics.¹⁴

In this letter, we report single crystals with a nominal formula of $(\text{K}_{0.45}\text{Na}_{0.55})_{0.96}\text{Li}_{0.04}\text{NbO}_3$ (KNN4N) grown by a SFSSCG method, where small amount additives of Li_2CO_3 and Bi_2O_3 were used as the sintering aids. We show that the single crystals exhibit a large d_{33} of 689 pC/N. Moreover, the large contribution of non-180° domain motions to the strain response of the single crystals under high electric field yields an effective piezoelectric d_{33}^* of 967 pm/V, a nearly 300 pm/V increase over the low field piezoelectric coefficient of 689 pm/V.

In this study, Na_2CO_3 (99.8%), K_2CO_3 (99%), Li_2CO_3 (98%), and Nb_2O_5 (99.5%), from Sinapharm Chemical Reagent Co., Ltd., were used as starting materials, which were mixed and planetary ball milled for 6 h in ethanol using zirconia balls. After the calcination at 850 °C for 5 h, the powders were sand-milled with the addition of 0.25 mol. % of Li_2CO_3 (98%) and 0.25 mol. % of Bi_2O_3 (99.99%, Shanghai Lingfeng Chemical Reagent, Co., Ltd.) for 2 h. The powders obtained were pressed into disks of 25 mm in diameter and 2–3 mm in thickness, followed by a cold isostatic pressing at 200 MPa. The samples were sintered in air at 1080 °C for 10 h. As shown in Fig. 1(a), large single crystals were obtained. They were oriented and polished to rectangular shape of about 0.5 mm thick for characterization.

The chemical compositions of the grown single crystals were examined by an X-ray fluorescence analyzer (XRF, AXIOS, PANalytical B.V., Netherland). The X-ray diffraction

^{a)} Authors to whom correspondence should be addressed. Electronic addresses: qb_yang@mail.sic.ac.cn and yxli@mail.sic.ac.cn

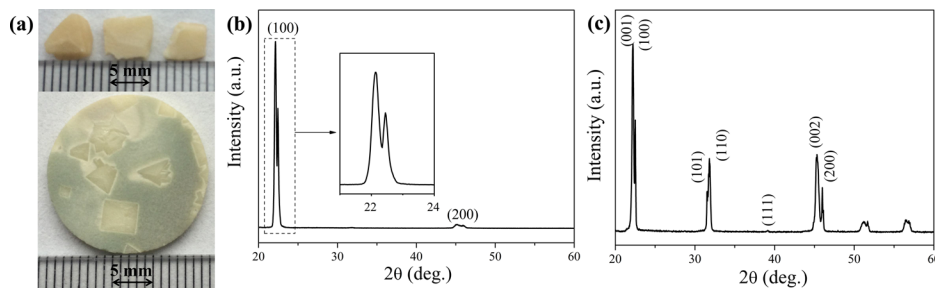


FIG. 1. (a) Photographs of the samples and the picked-out single crystals; (b) X-ray diffraction patterns of (100)-oriented KNL4N single crystals; and (c) the crushed single crystal powders.

of the (100)-oriented single crystals was examined using the Bruker D8 Discover high resolution X-ray diffraction (HRXRD) system in the Micro-area mode. The crystalline structures of the crushed single crystal powders were determined by an X-ray diffractometer (XRD, Bruker D8 Advance, Germany) in 2θ angle of 20° – 60° with Cu- $K\alpha$ radiation. Silver paste coated on the surfaces was fired at 700°C for 30 min to form the electrodes for electrical characterization. The temperature-dependent dielectric constant (ϵ_r) and dielectric loss ($\tan \delta$) were measured by an impedance analyzer (Wayne Kerr 6500B, UK) equipped with a temperature chamber. For piezoelectric properties' characterization, the crystals were poled for 30 min at room temperature under a DC electric field of 30 kV/cm. After aging for 24 h, the piezoelectric coefficient d_{33} was acquired using a Berlincourt-type quasi-static d_{33} meter (ZJ-3A, Institute of Acoustics, Beijing, China). The temperature dependence of d_{33} was characterized from 25°C to 500°C . The data were obtained at each temperature point after the temperature was stabilized for 30 min. The electrical polarization (P - E loops) and strain (S - E curves) were measured at 10 Hz and room temperature using a ferroelectric test system (Precision Premier II, Radiant Technologies, Inc., USA).

Fig. 1(a) presents photographs of the single crystals grown by the SFSSCG method. The crystals are not transparent which is caused by the presence of small pores inside, likely originated from the rapid growth of the crystals. Their largest size is $6\text{ mm} \times 5\text{ mm} \times 2\text{ mm}$. The crystals grown by the SFSSCG method are in rectangular or triangular shapes, indicating that the crystal growth is induced by two-dimensional (2D) nucleation rather than diffusion controlled mechanism.¹⁵ The chemical compositions of the grown single crystals were examined by the XRF technique. Since the light elements like Li cannot be directly measured by XRF, the compound is formulated as $[(\text{K}_{0.405}\text{Na}_{0.595})_{0.995-x}\text{Li}_x\text{Bi}_{0.005}]\text{NbO}_3$ ($0 < x < 0.04$) according to the measured K/Na ($\sim 68\%$) and Bi/Nb ($\sim 0.5\%$) ratios. Figs. 1(b) and 1(c) show the X-ray diffraction patterns of the (100)-orientated single crystals and the crushed crystal powders, respectively. Two peaks, e.g., (100) and (200), can be seen in Fig. 1(b), which shows that the samples are indeed single crystals. The inset presents an enlarged XRD pattern in a 2θ range of 21° – 24° , revealing that the (100) “peak,” in fact, consists of two peaks. This phenomenon has also been observed by Deng *et al.*,¹⁶ which is caused by the multi-domain feature in the ferroelectric crystals. The powder XRD pattern exhibits pure orthorhombic perovskite phase without detectable secondary phase (Fig. 1(c)). It is worth noting that the (001) and (100) peaks are much higher than others, while in the non-

textured ceramic cases, the (101) and (110) should be the highest.^{17–19} (001) and (100) faces are the low-energy cleavage faces for the KNN-based single crystals. During the crushing process, many (001) and (100)-oriented small plates will be produced, which will thus strengthen the intensities of the (001) and (100) peaks, as observed in Fig. 1(c).

The temperature dependence of dielectric properties of the KNL4N single crystals measured at 100 kHz is shown in Fig. 2. The dielectric data display two anomalies, at about 83°C and 432°C , respectively. The enlarged lower temperature peak is also presented in the inset, corresponding to the orthorhombic to tetragonal (O-T) phase transition at 83°C . Hence, the crystals have an orthorhombic structure at room temperature, which is consistent with the XRD data in Fig. 1(c). The peak at higher temperature (432°C) is interpreted as the ferroelectric tetragonal to paraelectric cubic (T-C) phase transition. The dielectric loss ($\tan \delta$) is less than 0.1 when the temperature is up to 278°C , indicating the potential of KNL4N single crystals for high temperature application. Fig. 3 presents the temperature dependence of d_{33} of the KNL4N single crystals. There are two sharp decreases observed at the temperature range of 65 – 75°C and 420 – 440°C . Comparing with Fig. 2, it can be concluded that these two decreases are related to the O-T and T-C phase transitions, respectively. The slightly higher O-T transition temperature $T_{\text{O-T}}$ (83°C) in Fig. 2 than that in Fig. 3 is likely caused by the thermal hysteresis of the O-T transition during the continuous heating of crystals in the dielectric measurement. The data reveal that d_{33} at room temperature can reach 689 pC/N. This value is much larger than that of the KNN-based materials reported in the literatures, including non-textured ceramics, textured ceramics, and single crystals.^{1,2,17,20,21} One reason for such a high d_{33} value in the KNL4N crystals is the lower $T_{\text{O-T}}$ ($\sim 83^\circ\text{C}$ in

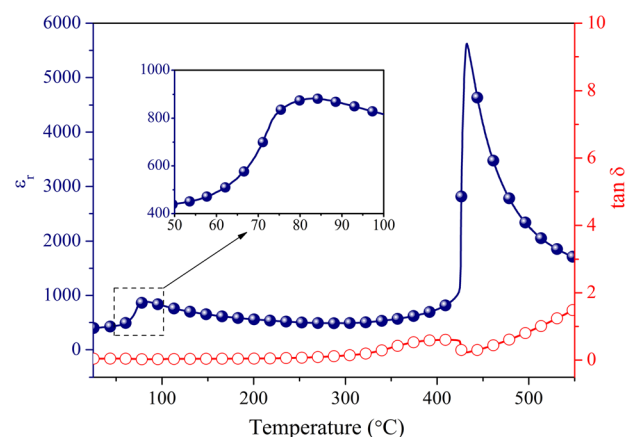


FIG. 2. Dielectric constant and dielectric loss as a function of temperature for KNL4N single crystals, measured at 100 kHz.

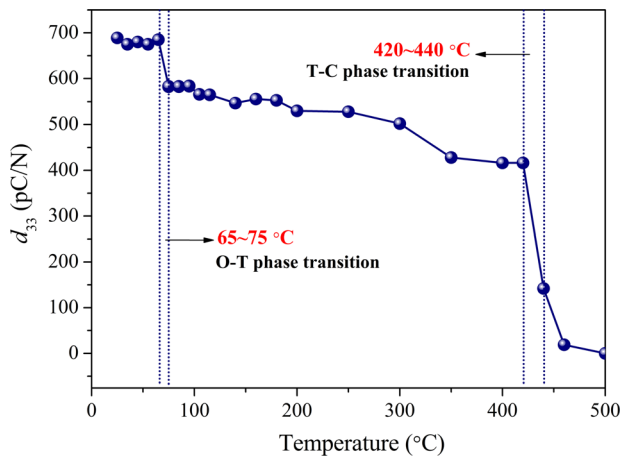
FIG. 3. Temperature dependence of piezoelectric coefficient d_{33} .

Fig. 2) in the crystals studied here. Using the Bridgman method, Chen *et al.*²⁰ grew Li-doped KNN single crystals which show a d_{33} of 405 pC/N, where the T_{O-T} is 192 °C, as shown in Table I. It was observed that, for Li-doped KNN ceramics, the lower the T_{O-T} temperature is, the larger the d_{33} will be, due to the easy polarization rotation with phase coexistence near O-T phase boundary.^{19,22} The T_{O-T} is 83 °C in our study, which is much lower than 192 °C of the crystals by Chen *et al.* Therefore, the d_{33} in our study is much larger.

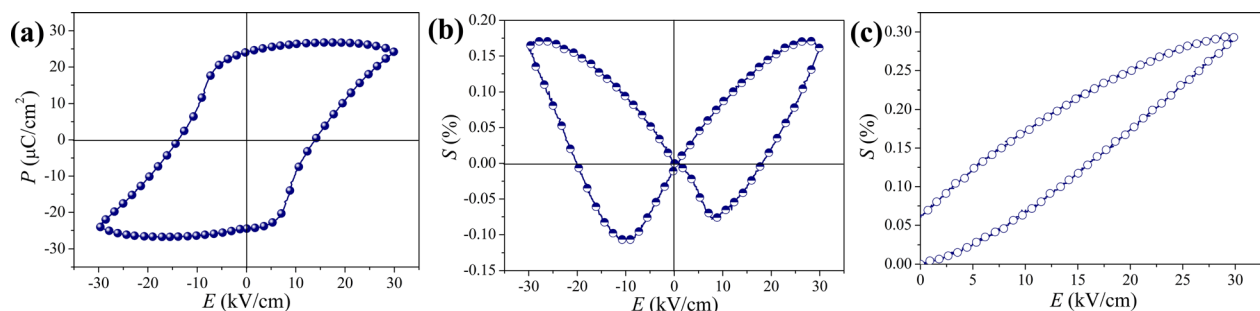
Fig. 4(a) shows the P - E loop of the KNL4N single crystals measured at 10 Hz and room temperature. The samples exhibit a typical square-like normal ferroelectric loop, with a high remnant polarization (P_r) of 24.1 $\mu\text{C}/\text{cm}^2$ and a coercive field (E_c) of 13.9 kV/cm. No obvious leakage current contribution can be observed in the P - E loop, indicating lower ionic vacancies in the crystals compared with those grown by the Bridgman method.²⁰ The bipolar electric field-induced strain curve of the KNL4N single crystals is shown

in Fig. 4(b). A butterfly shape is observed, which is a characteristic of a typical ferroelectric material. The curve is not perfectly symmetric, which could be caused by the electric field-induced polarization during the measurement. Large negative strain (defined as the absolute value of the lowest strain) of more than 0.1% is shown in Fig. 4(b), revealing the existence of irreversible non-180° domain switches in the single crystals.^{18,23} Ferroelectric materials are well known for exhibiting non-linear responses because of domain contributions to the polarization and strain switches.^{24,25} In order to characterize the effective piezoelectric coefficient d_{33}^* ($S_{\text{max}}/E_{\text{max}}$) under high electric fields, the unipolar strain response was measured, and one typical example is presented in Fig. 4(c). The curve is hysteretic with a large maximum unipolar strain of 0.29% at an electric field of 30 kV/cm. The d_{33}^* thus deduced is as large as 967 pm/V, originated from both the lattice distortion and the switching of non-180° domains.¹⁸

Table I summarizes the piezoelectric properties and Curie temperatures (T_C) of some high-performance piezoceramics and single crystals reported in the literatures recently. Wu *et al.*^{17,26} designed a new rhombohedral-tetragonal (R-T) phase boundary in KNN-based ceramics by doping, which markedly enhanced the piezoelectric properties in 0.96($\text{K}_{0.48}\text{Na}_{0.52}$)($\text{Nb}_{0.95}\text{Sb}_{0.05}$) O_3 -0.04 $\text{Bi}_{0.5}$ ($\text{Na}_{0.82}\text{K}_{0.18}$) ZrO_3 ($d_{33} = 490$ pC/N) and 0.96($\text{K}_{0.4}\text{Na}_{0.6}$)($\text{Nb}_{0.96}\text{Sb}_{0.04}$) O_3 -0.04 $\text{Bi}_{0.5}\text{K}_{0.5}$ ($\text{Zr}_{0.9}\text{Sn}_{0.1}$) O_3 ($d_{33} = 460$ pC/N, $d_{33}^* = 707$ pm/V) ceramics. (K, Na, Li)(Nb, Ta) O_3 :Mn (KNNTL:Mn) single crystal was grown by top-seeded solution growth (TSSG) method,²¹ which showed d_{33} of 630 pC/N and d_{33}^* of 870 pm/V. In our study, $\langle 100 \rangle$ -oriented KNL4N single crystals grown by the SFSSCG method exhibit d_{33} of 689 pC/N, and d_{33}^* of 967 pm/V. The d_{33} is the largest among the listed KNN-based materials and is much larger than the PZT4 ceramics.¹ In addition, the T_C of the single crystals is 432 °C,

TABLE I. Piezoelectric properties of KNL4N single crystals and comparison with other high-performance lead-based and lead-free piezoelectric materials (SC = single crystal).

Sample	d_{33} (pC/N)	d_{33}^* (pm/V)	T_C (°C)	References
PZT4 ceramic	410	700	250	1
0.96($\text{K}_{0.48}\text{Na}_{0.52}$)($\text{Nb}_{0.95}\text{Sb}_{0.05}$) O_3 -0.04 $\text{Bi}_{0.5}$ ($\text{Na}_{0.82}\text{K}_{0.18}$) ZrO_3 ceramic	490	...	227	17
0.96($\text{K}_{0.4}\text{Na}_{0.6}$)($\text{Nb}_{0.96}\text{Sb}_{0.04}$) O_3 -0.04 $\text{Bi}_{0.5}\text{K}_{0.5}$ ($\text{Zr}_{0.9}\text{Sn}_{0.1}$) O_3 ceramic	460	707	246	26
(K, Na, Li)(Nb, Ta) O_3 :Mn SC	630	870	235	21
0.95 $\text{K}_{0.5}\text{Na}_{0.5}\text{NbO}_3$ -0.05 LiNbO_3 SC	405	...	426	20
KNL4N SC	689	967	432	This work

FIG. 4. (a) P - E hysteresis loop, (b) bipolar, and (c) unipolar electrical field induced strain curves of KNL4N single crystals, measured at 10 Hz and room temperature.

which is also a high value compared with other lead-free piezoelectric materials.

In summary, lead-free piezoelectric single crystals with a nominal formula of $(\text{K}_{0.45}\text{Na}_{0.55})_{0.96}\text{Li}_{0.04}\text{NbO}_3$ (KNL4N) were grown by a seed-free solid-state crystal growth (SFSSCG) method. The crystals with the orthorhombic symmetry at room temperature are transferred to tetragonal and cubic at 83 °C and 432 °C, respectively. The single crystals possess a large d_{33} of 689 pC/N and a high d_{33}^* of 967 pm/V, due to the highly aligned domains and the low $T_{\text{O-T}}$ to the room temperature which facilitates the non-180° domain wall contribution to the piezoelectric response. Besides the development of lead-free single crystals with exceptionally high d_{33} , the results reported in this letter also demonstrate that SFSSCG method is a practical and economical way to fabricate high-performance lead-free piezoelectric crystals.

This work was supported by the National Natural Science Foundation of China (NSFC, Nos. 51332009 and 51172257), National Basic Research Program of China 973-Projects (2012CB619406), the CAS/SAFEA International Partnership Program for Creative Research Teams, and Science and Technology Commission of Shanghai Municipality (15ZR1445400). Y.L. appreciates the financial support from the Australian Research Council in the form of Future Fellowship. Many thanks go to Professor Jiwei Zhai of Tongji University for kind help on ferroelectric measurements.

¹Y. Saito, H. Takao, T. Tani, T. Nonoyama, K. Takatori, T. Homma, T. Nagaya, and M. Nakamura, *Nature* **432**, 84 (2004).

²Z. Q. Zhang, J. Yang, Z. F. Liu, and Y. X. Li, *J. Alloys Compd.* **624**, 158 (2015).

³S. J. Zhang, S. M. Lee, D. H. Kim, H. Y. Lee, and T. R. Shrout, *J. Am. Ceram. Soc.* **91**, 683 (2008).

⁴K. S. Moon, D. Rout, H. Y. Lee, and S. J. L. Kang, *J. Cryst. Growth* **317**, 28 (2011).

- ⁵S. J. L. Kang, J. H. Park, S. Y. Ko, and H. Y. Lee, *J. Am. Ceram. Soc.* **98**, 347 (2015).
- ⁶S. Y. Choi and J. H. Jeon, *Adv. Powder Technol.* **22**, 383 (2011).
- ⁷P. W. Rehrig, G. L. Messing, and S. Trolier-McKinstry, *J. Am. Ceram. Soc.* **83**, 2654 (2000).
- ⁸J. G. Fisher, A. Bencan, J. Godnjavec, and M. Kosec, *J. Eur. Ceram. Soc.* **28**, 1657 (2008).
- ⁹H. Ursic, A. Bencan, M. Skarabot, M. Godec, and M. Kosec, *J. Appl. Phys.* **107**, 033705 (2010).
- ¹⁰J. Yang, Q. B. Yang, Y. X. Li, and Y. Liu, *J. Eur. Ceram. Soc.* **36**, 541 (2016).
- ¹¹J. M. Saldana, B. Mullier, and G. A. Schneider, *J. Eur. Ceram. Soc.* **22**, 681 (2002).
- ¹²C. Wang, Y. D. Hou, H. Y. Ge, M. K. Zhu, and H. Yan, *J. Eur. Ceram. Soc.* **30**, 1725 (2010).
- ¹³M. H. Jiang, C. A. Randall, H. Z. Guo, R. Tu, Z. F. Gu, G. Cheng, X. Y. Liu, J. W. Zhang, and Y. X. Li, *J. Am. Ceram. Soc.* **98**, 2988 (2015).
- ¹⁴Y. L. Li, C. Hui, M. J. Wu, Y. X. Li, and Y. L. Wang, *Ceram. Int.* **38**, S283 (2012).
- ¹⁵M. K. Kang, D. Y. Kim, and N. M. Hwang, *J. Eur. Ceram. Soc.* **22**, 603 (2002).
- ¹⁶H. Deng, H. W. Zhang, X. Y. Zhao, C. Chen, X. A. Wang, X. B. Li, D. Lin, B. Ren, J. Jiao, and H. S. Luo, *CrystEngComm* **17**, 2872 (2015).
- ¹⁷X. P. Wang, J. G. Wu, D. Q. Xiao, J. G. Zhu, X. J. Cheng, T. Zheng, B. Y. Zhang, X. J. Lou, and X. J. Wang, *J. Am. Chem. Soc.* **136**, 2905 (2014).
- ¹⁸T. Zheng, J. G. Wu, D. Q. Xiao, J. G. Zhu, X. J. Wang, and X. J. Lou, *J. Mater. Chem. A* **3**, 1868 (2015).
- ¹⁹Y. P. Guo, K. Kakimoto, and H. Ohsato, *Appl. Phys. Lett.* **85**, 4121 (2004).
- ²⁰K. Chen, G. S. Xu, D. F. Yang, X. F. Wang, and J. B. Li, *J. Appl. Phys.* **101**, 044103 (2007).
- ²¹X. Q. Huo, R. Zhang, L. M. Zheng, S. J. Zhang, R. Wang, J. J. Wang, S. J. Sang, B. Yang, and W. W. Cao, *J. Am. Ceram. Soc.* **98**, 1829 (2015).
- ²²J. H. Gao, S. Ren, L. Zhang, Y. S. Hao, M. X. Fang, M. Zhang, Y. Dai, X. H. Hu, D. Wang, L. S. Zhong, S. T. Li, and X. B. Ren, *Appl. Phys. Lett.* **107**, 032902 (2015).
- ²³J. Fu and R. Z. Zuo, *Acta Mater.* **61**, 3687 (2013).
- ²⁴Q. M. Zhang, W. Y. Pan, S. J. Jang, and L. E. Cross, *J. Appl. Phys.* **64**, 6445 (1988).
- ²⁵D. Damjanovic and M. Demartin, *J. Phys. D: Appl. Phys.* **29**, 2057 (1996).
- ²⁶T. Zheng, J. G. Wu, D. Q. Xiao, J. G. Zhu, X. J. Wang, L. P. Xin, and X. J. Lou, *ACS Appl. Mater. Interfaces* **7**, 5927 (2015).